ChemComm

Accepted Manuscript

This is an *Accepted Manuscript*, which has been through the Royal Society of Chemistry peer review process and has been accepted for publication.

Accepted Manuscripts are published online shortly after acceptance, before technical editing, formatting and proof reading. Using this free service, authors can make their results available to the community, in citable form, before we publish the edited article. We will replace this *Accepted Manuscript* with the edited and formatted *Advance Article* as soon as it is available.

You can find more information about *Accepted Manuscripts* in the **Information for Authors**.

Please note that technical editing may introduce minor changes to the text and/or graphics, which may alter content. The journal's standard **Terms & Conditions** and the **Ethical guidelines** still apply. In no event shall the Royal Society of Chemistry be held responsible for any errors or omissions in this *Accepted Manuscript* or any consequences arising from the use of any information it contains.

Journal Name

Dynamic Article Links ▶

ARTICLE TYPE

Novel Co@Au structure formed in bimetallic core@shell nanoparticles

Alvaro Mayoral,*[a] Daniel Llamosa[b] and Yves Huttel*[b]

5 **Core@shell Co@Au nanoparticles of around 8 nm have been produced by inert gas condensation method, revealing for the first time that most of the nanoparticles present an icosahedral shape in agreement with the theoretical prediction. Additionally, we report the existence of a novel** 10 **morphology which consists of a Co icosahedron surrounded by *fcc* Au facets, reported here for the first time.**

It is well-known that the properties of matter at the nanoscale significantly differ from the bulk. Growing nanoparticles has attracted a great interest in fundamental science and for industrial 15 applications in different areas such as catalysis, magnetism, optics or electronics[1-5]. In addition to the unique properties directly related to the reduced size, structural and compositional parameters can be, at least to some extent, partially tuned conferring more functions to a single nanoparticle. In this 20 context, the formation of nanoalloys or bimetallic nanoparticles is crucial for the development of multifunctional materials. Nanoalloys can adopt a variety of shapes and the atomic structural conformation can be modified depending on their size and composition[6], adopting crystalline structures (fragments of 25 the bulk material), disordered structures, decahedra (dh), icosahedra (ih) or polyhedra[6]. On the other hand, in the nanoparticles the chemical arrangement of the elements can display an intermixing[7], a core@shell[8, 9] structure or a Janus disposition[10]. Thus, alloys formed by magnetic metals such as Co 30 or Ni and noble metals as Au, Ag or Pt have gained an enormous interest as they exhibit the magnetism from the Co or Ni and optical or catalytical properties of the Au[11, 12] for example. Core@shell Co@Au nanoparticles have been proposed for biomedical applications in the magnetotherapy taking advantage 35 of the magnetic core (Co) that is protected from the oxidation by a shell of Au which in addition, confers biocompatibility, optical properties and the benefits of easy functionalization of the nanoparticles.

There is a variety of methods for the production of metallic 40 nanoparticles (NPs) composed of more than one element, the chemical procedures being the most common approaches[13-16] with the possibility to obtain core@shell[17, 18] structure and polyhedral geometries. On the other hand, physical methods tend to allow a better control over the size distribution and shape of 45 the nanoparticles (NPs), making them more suitable when such properties are critical for a desired application. Inert gas aggregation[8, 9], where targets of the desired components are magnetron-sputtered, in order to extract the atoms, which

aggregate and are finally deposited on a substrate is probably the 50 most widely used method.

Until recently, the detailed characterization of such small materials by Transmission Electron Microscopy (TEM) has been extraordinarily difficult and not very precise. However, with the implementation of the spherical aberration correctors (C_s) sub-55 ̊angstrom resolution can be commonly achieved providing sharp and clear images that allow a precise identification of the atomic columns or even single isolated atoms[19-22]. Moreover, the combination of these corrected instruments operated in scanning transmission mode (STEM) using high angle annular dark field 60 detectors (HAADF) facilitate the direct interpretation of the data acquired if the Z difference is high enough, which has converted C_s-corrected STEM-HAADF microscopy in a unique method for the observation of metals in light supports[11, 23, 24] or the interphases in metallic nanoparticles[8, 25]. In the current work C_s-65 corrected STEM-HAADF has been used to analyze bimetallic core@shell Co@Au NPs produced by a modified gas aggregation approach called Multiple Ion Cluster Source (MICS) that allows the one-step generation of nanoparticles with well-controlled size, chemical composition and structure[26, 27]. The experimental 70 observations presented here are quite remarkable as they reveal a novel structure that some of the Co@Au NPs adopted. In addition to this new conformation, the results here reported corroborate the calculations proposed by Bochicchio and Ferrando[28] who predicted that the icosahedron structure is the most favorable 75 configuration for core@shell Co@Au nanoparticles in terms of energy.

Core-shell nanoparticles are produced, where the final element distribution can be tuned by modifying the position of the magnetrons within the MICS[27, 29]; therefore, the system employed 80 here was set in order to favour the formation of a Co core and an Au shell. This distribution is also chemically favoured as the Au presents a larger atomic radius together with smaller cohesive and surface energies that favour the noble metal surface segregation[28, 30-33]. Taking advantage of the atomic resolution images which can 85 be acquired simultaneously with chemical information data with high spatial-resolution it has been possible to determine a relationship between geometry and element ordering. Here, Co@Au nanoparticles have been produced with a very good size distribution presenting an average size of 7.5 - 8 nm in diameter. 90 The high control of the size distribution is illustrated in Fig. 1a, where several NPs are shown. More interestingly than the great control of the particle size is the structural confirmation and elemental disposition that the NPs exhibit; three different types of
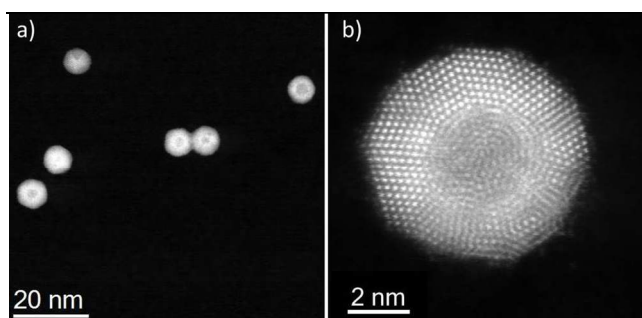
Fig.1 (a) C$_s$-corrected STEM-HAADF image of several, 7.5 - 8 nm diameter Co@Au nanoparticles. (b) C$_s$-corrected STEM-HAADF image of a Co icosahedron coated by Au.

nanoparticles have been observed in the system. Pure Au
5 decahedron (≈ 20% of them, Fig. S1), which is very typical for Au NPs[6] and it can be attributed to the aggregation of Au atoms and ions of the super-saturated gas originated from the magnetron loaded with Au. Secondly, and the most abundant (≈ 60%) type of NPs are pure Icosahedral nanoparticles (Fig. S2). Bochicchio
10 and Ferrando[28] predicted that the Ih structure is the most stable conformation for core@shell Co@Au NPs. Although the theoretical study of Bochicchio and Ferrando was focused on smaller NPs (≈ 3 nm diameter); here we experimentally corroborate the theoretical results and further extend the stability
15 of such structure up to 8 nm (Fig. S2). For this case, the entire crystal is an icosahedron where the atoms in the nuclei are Co and the subsequent layers are formed by Au atoms. The third type of NPs that has been observed is shown in Fig. 1b and Fig. S3, where a particular conformation is observed and reported here for
20 the first time. The lower contrast observed in the center of the NPs of Fig. 1b and S3 suggests a difference in the atomic number of the atoms of the core with respect to the atoms of the shell. The core is attributed to a Co rich zone as confirmed by energy electron loss spectroscopy (EELS). Fig. 2a displays the
25 compositional map corresponding to the Co-L$_{3,2}$ edge superimposed on the high-resolution image which perfectly fits with the less brighter zone of the core of the nanoparticle. The extracted EELS spectrum, Fig. 2b, shows the Co-L$_{3,2}$ edge and the absence of oxygen signal proving the good protection of the
30 Au from the Co oxidation.

Fig. 3a depicts the inverse FFT image of the Co core and the corresponding FFT diffractogram is displayed in Fig. 3b, while, for the sake of comparison, an ideal FFT diffractogram of a perfect icosahedron is shown in Fig. 3c (all of them orientated
35 along their 5-fold axis). It is clearly deduced that the Co core of the experimentally observed Co@Au nanoparticle has an icosahedron structure as predicted by Bochicchio and Ferrando[28].
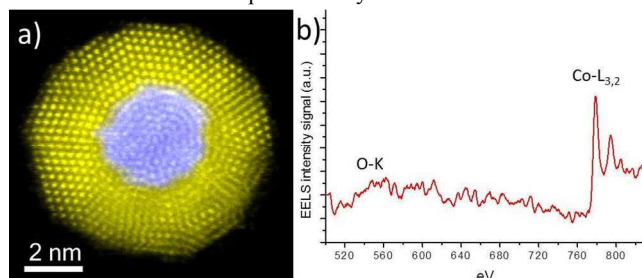

Fig. 2 (a) Atomic resolution image of the Co@Au nanoparticle with the
40 Au artificially colored (yellow) and the superimposed Co-L$_{3,2}$ signal map (blue). (b) EELS spectrum extracted from the core, blue part of Fig. 2a with the Co-L$_{3,2}$ edge.
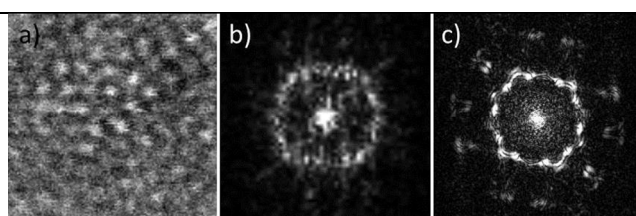

Fig. 3 (a) FFT filtered image of the Co core. (b) Corresponding FFT
45 diffractogram of (a). (c) Corresponding FFT from a pure icosahedron along its five-fold axis.

In their study, these authors demonstrated that the lowest-energy configuration for a nanoparticle of around 3 nm diameter with a Co core of 4 layers (equal to 147 Co atoms) and an Au shell of 8
50 layers is an icosahedron. For the present case the nanoparticles are larger since they present a diameter of around 8 nm with a core of 3.3 nm and an external Au shell of 8 layers. While Bochicchio and Ferrando predicted an Au shell with an icosahedral structure, here for much larger nanoparticles it is
55 proved that such conformation is stable into a great extent; however, in addition to this it has been also observed that the outer Au shell exhibits distortions from the theoretically proposed icosahedron.

For the present case the Co core, with icosahedral shape, is
60 oriented along the 5-fold axis; it is well-known that metal nanoparticles in the range of 2 - 10 nm are typically multi-twinned decahedral or icosahedral structures formed by non-space filling 10 or 20 tetrahedra respectively. In order to finally complete these forbidden structures each of the units need to be
65 strained[6, 34-36] to close the remaining gaps; however, for the case of bimetallic nanoparticles chemical ordering also needs to be taken into account in the final morphology. This is the case of the current Co@Au system; no bimetallic decahedra or *face-centered cubic structure* (*fcc*) NPs has been observed and only core@shell
70 icosahedra were formed, as it has been energetically predicted by Bochicchio and Ferrando[28]. Fig. 4a presents the 2-dimensional projection of an icosahedron with a perfectly centered Co core surrounded by an Au shell that is composed by 10 crystallographic *fcc* domains linked by twin planes. Fig. 4b shows
75 the experimental data collected orientated along the same direction. As can be observed there are some similarities between the ideal icosahedron and the structure where 10 *fcc* domains can be observed. Furthermore, no projected image of a purely icosahedron structure would lead to the observation of the 10 *fcc*
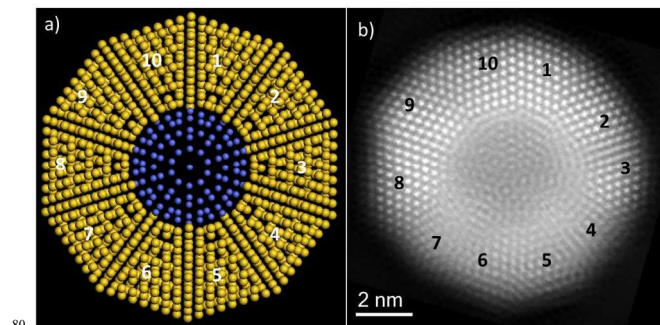

80
Fig. 4 (a) Schematic model of a sliced icosahedral core fully occupied by Co atoms (blue) and a shell formed by 10 *fcc* projected domains formed by Au atoms (yellow). (b) Aberration-corrected STEM-HAADF image of the corresponding Co@Au nanoparticle. In both figures the 10 Au *fcc*
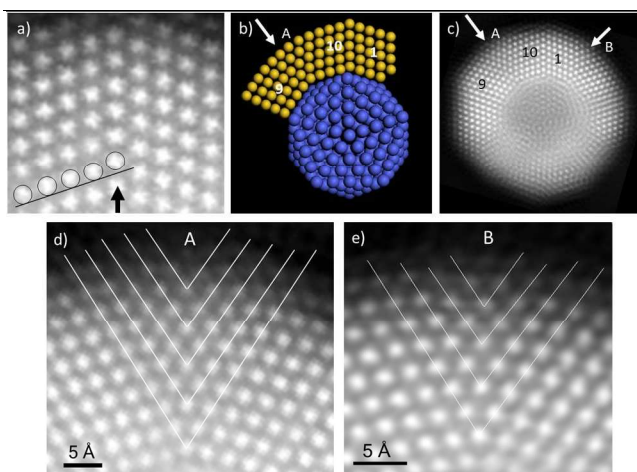85 domains are numbered.

Fig. 5 (a) Cs-corrected STEM-HAADF image of the magnified region displaying a twin plane. The atomic positions are marked by black circles; the atomic column belonging to the twin plane is denoted by a black
5 arrow pointing into the direction where these atomic columns are displaced. (b) Atomistic model of the Co core (blue) and Au shell (yellow), with one of the intergrowths marked (arrow) as A. The *fcc* facets are numbered. (c) C$_s$-corrected STEM-HAADF image of a core@shell nanoparticle where two intergrowths positions are marked as
10 "A" and "B". (d) and (e) Zoom of the triangular junction units.

domains as presented here which suggests the formation a new structure with an icosahedron in the center and pure Au *fcc* facets encapsulating it. By observing an ideal icosahedron on its 5-fold zone axis the projected 2-dimensional image would exhibit 10
15 facets (see model S4) and each of these facets may act as growing point for the adsorption of the gold atoms leading into the formation of 10 different *fcc* domains. However, due to the high strain that the tetrahedra present in these materials in order to fill the space[35, 36] the growing facets would be also highly strained in
20 order to completely cover the Co surface. In order to measure the strain of decahedra and icosahedra, different approaches have been reported. Johnson *et al*. used geometrical phase analysis (GPA) to describe the presence of a disclination and shear gradients together with the importance of elastic anisotropy[34] in a
25 35 nm (diameter) Au nanoparticle; however, this method to measure the strain can be only applied to relatively large nanoparticles where an area free of defects can be used as reference. For icosahedra or very small nanoparticles the interatomic distances have been manually measured for each
30 column in order to determine the strain present in the particles. Herein, the units perfectly orientated perpendicular to the electron beam were used in order to measure the atomic (columns) distances between adjacent atoms (Fig. S5). In this case, the atomic columns that take part in the twin planes were not taken
35 into account as the atoms are displaced from their theoretical positions by ≈ 11% through the direction marked by the arrow in Fig. 5a. The interatomic distances measured did not reveal any tendency (Fig. S5) as it has been reported for single metal decahedra and icosahedra[35, 36] measuring a mean d$_{111}$ = 2.642 Å.
40 This reveals that no strain is present in the outer part of the nanoparticle formed by single crystal units. Such result is coherent with an intergrowth that would fill the gaps between some of the *fcc* structures. An atomistic simulation is displayed in Fig. 5b; the Co icosahedron appears in blue color and the Au in
45 yellow. For simplicity only top part has been built, units

numbered as 9, 10 and 1 (Fig. 5c), and the "linking units" marked by an arrow denoted as "A & B". These two intergrowths (A and B, Fig. 5c) exhibit triangular shape of approximately 2 nm (measured in the external surface) for both cases and with an
50 angle of 66° for A and 56° for B (Fig. 5d and 5e respectively). The two cases observed in this nanoparticle resembles to a chevron defect which has been previously reported in Au[37] and Ag[38] intersections. The junction denoted as "A" links two <110> units which are rotated to each other by 149°; meanwhile unit
55 "B" links another two <110> units rotated by 141°. The two intergrowths, also along the 110 zone axis are responsible for closing the gap of the nanoparticle and releasing the strain that would be present if only the 10 facets were forming the shell.

Conclusions

60 In summary, bimetallic core@shell Co@Au nanoparticles have been produced by Multiple Ion Cluster Source inert gas condensation method. The elemental distribution has been analyzed by analytical methods (EELS and EDS) confirming the presence of both metals in most (80%) of the single
65 nanoparticles. As theoretically predicted by Bochicchio and Ferrando no decahedral nanoparticles were observed containing both metals and they always adopted icosahedral shapes or a novel structure presented here for the first time. The novel structure consisted on icosahedra made of pure Co that is coated
70 by 10 pure Au *fcc* facets along the <110> direction which are linked to each other by twin planes. In addition to the 10 facets, two intergrowths are present which are responsible for releasing the strain that the nanoparticle would present.

Notes and references

*^{a} Laboratorio de Microscopias Avanzadas (LMA), Nanoscience Institute of Aragon (INA), University of Zaragoza, Mariano Esquillor, Edificio I+D, 50018, Zaragoza, Spain. Fax: +34 976 762 776; Tel: +34
85 876555368XXXX; E-mail: amayoral@unizar.es*
^{b} Instituto de Ciencia de Materiales de Madrid, Consejo Superior de Investigaciones Científicas (CSIC), Sor Juana Inés de la Cruz, 3, 28049, Madrid, Spain. E-mail:huttel@icmm.csic.es
† Electronic Supplementary Information (ESI) available: [Experimental
90 part]. See DOI: 10.1039/b000000x/

1   G. Schmid, H. West, J. O. Malm, J. Bovin and C. Grenthe, *Chem.-Eur. J.*, 1996, **2**, 1099-1103.

2   V. Caps, S. Arrii, F. Morfin, G. Bergeret and J. L. Rousset, *Faraday
95   Discuss.*, 2007, **138**, 241-256.

3   M. Castrillon, A. Mayoral, C. Magen, J. G. Meier, C. Marquina, S. Irusta and J. Santamaria, *Nanotechnology*, 2012, **23**, 085601-085610.

4   M. Castrillon, A. Mayoral, A. Urtizberea, C. Marquina, S. Irusta, J. G. Meier and J. Santamaria, *Nanotechnology*, 2013, **24**, 505702-
100   505711.

5   A. N. Shipway, E. Katz and I. Willne, *Chem. Phys. Chem.*, 2000, **1**, 18-52.

6   A. Mayoral, H. Barron, R. Estrada-Salas, A. Vazquez-Duran and M. Jose-Yacaman, *Nanoscale*, 2010, **2**, 335-342.

7   M. M. Mariscal, A. Mayoral, J. A. Olmos-Asar, C. Magen, S. Mejia-Rosales, E. Perez-Tijerina and M. Jose-Yacaman, *Nanoscale*, 2011, **3**, 513-519.

8   A. Mayoral, S. Mejia-Rosales, M. M. Mariscal, E. Perez-Tijerina and M. Jose-Yacaman, *Nanoscale*, 2010, **2**, 2647-2651.

9   D. Llamosa-Perez, A. Espinosa, L. Martínez, E. Román, C. Ballesteros, A. Mayoral, M. García-Hernández and Y. Huttel, *J. Phys. Chem. C*, 2013, **117**, 3101-3108.

10   I. Parsina and F. Baletto, *J. Phys. Chem. C*, 2010, **114**, 1504-1511.

11   A. Corma, P. Concepcion, M. Boronat, M. J. Sabater, J. Navas, M. Jose-Yacaman, E. Larios, A. Posadas, M. A. Lopez-Quintela, D. Buceta, E. Mendoza, G. Guilera and A. Mayoral, *Nat. Chem.*, 2013, **5**, 775-781.

12   F. H. B. Lima, J. F. R. d. Castro and E. A. Ticianelli, *J. Power Sources*, 2006, **161**, 806-812.

13   T. Itakura, K. Torigoe and K. Esumi, *Langmuir*, 1995, **11**, 4129–4134.

14   M. Brust, M. Walker, D. Bethell, D. J. Schiffrin and R. J. Whyman, *J. Chem. Soc. Chem. Commun.*, 1994, 801.

15   M. J. Hostetler, C. J. Zhong, B. K. H. Yen, J. Anderegg, S. M. Gross, N. D. Evans, M. Porter and R. W. Murria, *J. Am. Chem. Soc.*, 1998, **120**, 9396–9397.

16   M. M. Mariscal, J. A. Olmos-Asar, C. Gutierrez-Wing, A. Mayoral and M. J. Yacaman, *Phys. Chem. Chem. Phys.*, 2010, **12**, 11785–11790.

17   I. Srnová-Šloufová, F. Lednický, A. Gemperle and J. Gemperlová, *Langmuir, 2000, 16 (25), pp 9928–9935*, 2000, **16**, 9928–9935.

18   S. J. Mejía-Rosales, C. Fernández-Navarro, E. Pérez-Tijerina, D. A. Blom, L. F. Allard and M. José-Yacamán, *J. Phys. Chem. C* 2007, **111**, 1256-1260.

19   P. E. Baston, N. Dellby and O. L. Krivanek, *Nature*, 2002, **418**, 617.

20   P. E. Baston, *Ultramicroscopy*, 2006, **106**, 1104.

21   Z. Y. Li, N. P. Young, M. D. Vece, S. Palomba, R. E. Palmer, A. L. Bleloch, B. C. Curley, R. L. Johnston, J. Jiang and J. Yuan, *Nature*, 2008, **451**, 46.

22   A. Mayoral, D. A. Blom, M. M. Mariscal, C. Guiterrez-Wing, J. Aspiazu and M. Jose-Yacaman, *Chem. Commun.*, 2010, **46**, 8758–8760.

23   A. Mayoral, T. Carey, P. A. Anderson, A. Lubk and I. Diaz, *Angew. Chem. Int. Ed.*, 2011, **50**, 11230–11233.

24   A. Mayoral, J. E. Readman and P. A. Anderson, *J. Phys. Chem. C*, 2013, **117**, 24485–24489.

25   D. Ferrer, D. A. Blom, L. F. Allard, S. Mejia, E. Perez-Tijerina and M. Jose-Yacaman, *J. Mater. Chem.*, 2008, **18**, 2442-2446.

26   L. Martínez, M. Díaz, E. Roman, M. Ruano, P. D. Llamosa and Y. Huttel, *Langmuir*, 2012, **28**, 11241-11249.

27   D. Llamosa, M. Ruano, L. Martínez, A. Mayoral, E. Roman, M. García-Hernández and Y. Huttel, *Nanoscale*, 2014, **6**, 13483-13486.

28   D. Bochicchio and R. Ferrando, *Phys. Rev. B*, 2013, **87**, 165435.

29   D. Llamosa, L. Martínez and Y. Huttel, *Dataset papers in Nanotechnology*, 2014, Article ID 584391.

30   C. Langlois, Z. L. Li, J. Yuan, D. Alloyeau, J. Nelayah, D. Bochicchio, R. Ferrando and C. Ricolleau, *Nanoscale*, 2012, **4**, 3381-3388.

31   L. L. Wang and D. D. Johnson, *J. Am. Chem. Soc.*, 2009, **131**, 14023–14029.

32   A. Rapallo, J. A. Olmos-Asar, O. A. Oviedo, M. Ludueña, R. Ferrando and M. M. Mariscal, *J. Phys. Chem. C*, 2012, **116**, 17210–17218.

33   S. Núñez and R. L. Johnston, *J. Phys. Chem. C*, 2010, **114**, 13255–13266.

34   C. L. Johnson, E. Snoeck, M. Ezcurdia, B. Rodríguez-González, I. Pastoriza-Santos, L. M. Liz-Marzán and M. J. Hÿtch, *Nature materials*, 2007, **7**, 120.

35   M. J. Walsh, K. Yoshida, A. Kuwabara, M. L. Pay, P. L. Gai and E. D. Boyes, *Nano Lett.*, 2012, **12**, 2027-2031.

36   D. Pohl, U. Wiesenhütter, E. Mohn, L. Schultz and B. Rellinghaus, *Nano Lett.*, 2014, **14**, 1776-1784.

37   T. Radetic, F. Lançon and U. Dahmen, *Phys. Rev. Lett.*, 2002, **89**, 085502-085501 - 085502-085504.

38   A. Mayoral, L. F. Allard, D. Ferrer, R. Esparza and M. Jose-Yacaman, *J. Mater. Chem.*, 2010, **21**, 893–898.